Transfer Learning-based Approach for Polsar Image Classification

Sai Gurav
University of Southern California, Los Angeles, California, United States

Aarya Shinde
University of Mumbai, Mumbai, Maharashtra, India

Bhakti Talele
Carnegie Mellon University, Pittsburgh, Pennsylvania, United States

Avinash Dhiran
University of Twente, Enscede, Overijssels, Netherlands

Samay Shetty
Rochester Institute of Technology, Rochester, New York, United States

Sayan Panja
University of Mumbai, Mumbai, Maharashtra, India

Varsha Turkar
Thakur Shyamnarayan Engineering College, Mumbai, Maharashtra, India

Yogesh Agarwadkar
InfiCorridor Solutions Pvt. Ltd. Mumbai, Maharashtra, India

Mugdha Agarwadkar
A.P Shah Institute of Technology, Mumbai, Maharashtra, India

ABSTRACT
Polarimetric Synthetic Aperture Radar (PolSAR) data presents significant advantages compared to optical remote sensing, particularly due to its capability to obtain consistent imagery irrespective of solar illumination or atmospheric conditions. Although optical satellites are proficient in frequent data acquisition, their utility is frequently hindered by cloud cover and reliance on sunlight. In contrast, PolSAR operates independently of radiance and possesses the ability to penetrate cloud layers, thereby facilitating dependable, all-weather, day-and-night observations. Nonetheless, the intricate nature of PolSAR data and the expertise required for its analysis have posed significant challenges to widespread adoption. To mitigate this issue, the current study proposes a user-centric land cover classification tool aimed at simplifying the classification and interpretation of ALOS2-PALSAR L-band imagery. The tool utilizes a Random Forest classifier, which has been trained on labelled data from Mumbai, to categorize five distinct land cover types—water, settlements, forests, wetlands, and mangroves—across five designated regions: Mumbai, New Delhi, Ahmedabad, San Francisco, and California. The classification accuracy across these locations varies from 65% to over 95%, indicative of regional discrepancies in landscape structure and land cover categories. The tool is scalable for additional training sets with the possibility of global classification coverage and different classification techniques in its final form. The tool provides segmented images along with the area estimates for each land cover class.

General Terms
Remote Sensing, Machine Learning, Image Processing, Geospatial Analysis

Keywords
PolSAR, Land cover classification, Random Forest, ALOS-2 PALSAR, Graphical User Interface

1. INTRODUCTION
In 1994, the first spaceborne imaging radar, SIR-C, was launched. This was a collaborative project between the U.S., Germany, and Italy, aimed at studying global environmental changes. Since then, space agencies including NASA, ESA, JAXA, and ISRO have launched numerous imaging radar missions, primarily

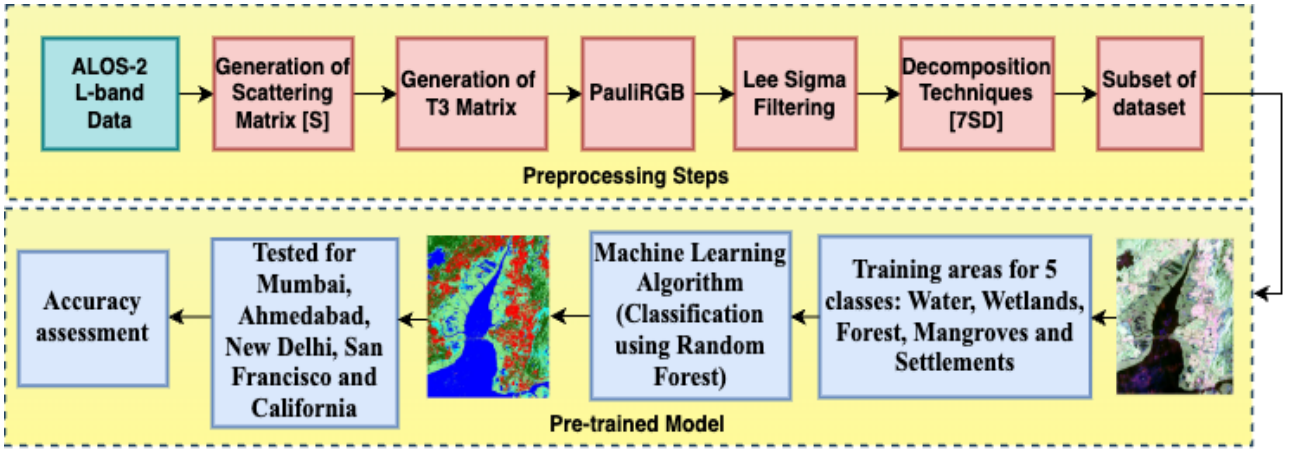

Fig 1: Development of RF Model to classify PALSAR data

aimed at surveillance, defense, environmental monitoring, and geospatial mapping. In 2015, ESA launched the Sentinel-1 C-band satellite, providing free access to its data. Initially, researchers relied on traditional classifiers to analyze this data for diverse remote sensing applications. The growing availability of freely accessible SAR datasets has recently accelerated the adoption of machine learning and deep learning techniques for land cover classification. However, microwave remote sensing data is inherently complex and demands a thorough understanding of the underlying physical principles. Such data plays a critical role in the development and validation of advanced classification algorithms [1]. This complexity has limited the widespread adoption of microwave remote sensing, particularly among non-expert users. The need for user-friendly interfaces in practical applications is highlighted by Hossain [2], who discusses the creation of MATLAB-based GUIs for remote sensing analysis. Building on these foundations, the methodology proposed in this paper integrates insights from Waske et al. [3] and Pal [4] to develop a robust, user-oriented classification tool. Researchers have explored various machine learning classifiers, including Support Vector Machine (SVM), Decision Tree, Neural Networks, and Random Forest—for land cover classification using polarimetric SAR data in remote sensing applications [5,6,7,8]. Random Forest (RF) is widely used for land cover classification in remote sensing due to its robustness, ability to reduce overfitting, and high classification accuracy. Its effectiveness stems from the ensemble learning approach, where multiple decision trees are created using the bagging technique [9,10,11]. However, the accuracy of RF models is heavily influenced by the choice of input features and hyperparameters [12,13]. In conventional approaches, feature selection is often performed arbitrarily, and hyperparameters, such as the number of trees in a Random Forest classifier, are typically determined through empirical trial-and-error, with 100 trees being a widely adopted configuration. Among various classifiers, Random Forest has consistently demonstrated superior classification accuracy [14,15]. In this study, the 7-component (7SD) target decomposition technique is employed, as it has been shown to outperform other decomposition methods in capturing detailed scattering characteristics [16, 17, 18]. Given its ability to effectively handle high-dimensional data and model complex, non-linear relationships, the Random Forest classifier is well-suited for processing ALOS2-PALSAR imagery [19].

Furthermore, Kotru et al. [20] introduced a generalized semantic segmentation framework utilizing ALOS2-PALSAR L-band fully polarimetric SAR data for land cover classification, proving its robustness across varying geographical contexts. Similarly, Varsha et al. [21] proposed a generalized machine learning model capable of classifying data acquired from ALOS2-PALSAR L-band, irrespective of geographical area, for the same land cover features. Complementing these efforts, Camargo et al. [22] conducted a comparative assessment of machine learning algorithms for land use and land cover mapping in the Brazilian tropical savanna using ALOS2-PALSAR data, underscoring the utility of polarimetric features in large-scale classification tasks.

2. METHODOLOGY

2.1 Dataset Description

The datasets employed in this study consist of ALOS2-PALSAR L-band fully polarimetric Synthetic Aperture Radar (PolSAR) imagery acquired over five geographic region-Mumbai, New Delhi, Ahmedabad, California, San Francisco. The datasets were obtained in quad-polarization mode, including HH(Horizontal-Horizontal), HV(Horizontal-Vertical), VV(Vertical-Vertical), and VH(Vertical-Horizontal) channels. The use of fully polarimetric SAR data enables detailed characteristics of scattering mechanism associated with urban settlements, water, vegetation, and wetlands.

The selected study regions represent heterogeneous environmental and urban conditions. Mumbai was selected as the primary training region because of its distinct geographical scenarios, coastal characteristics, and heterogenous land cover composition. The remaining dataset were employed to evaluate the transferability and generalization capabilities of the proposed classification approach.

2.2. Preprocessing

The preprocessing workflow adopted in this study is illustrated in Fig. 1. The raw data is used to generate the scattering matrix [S], containing the complex backscatter information from all polarization, which is subsequently transformed into a coherency matrix [T3].

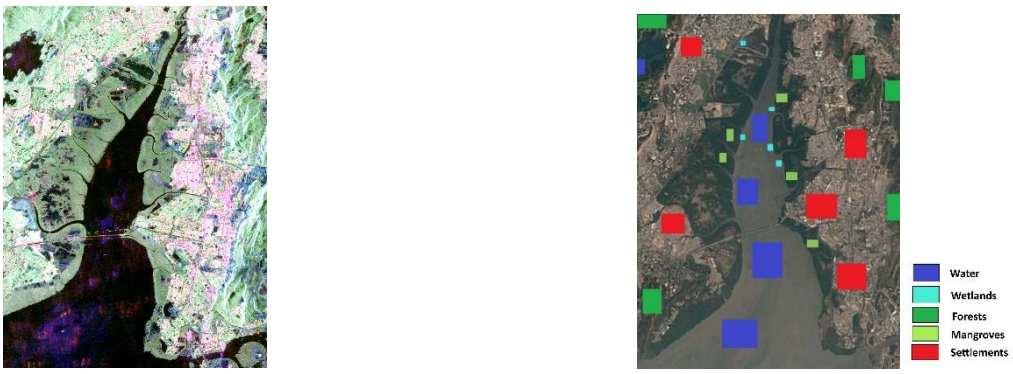

(a) (b)

Fig. 2: ALOS2-PALSAR L-Band Data for Mumbai: (a) Pauli RGB image, (b) Corresponding Google Earth image with training areas

The Pauli scattering vector used for coherency matrix generation is expressed as:

$$k_p = \frac{1}{\sqrt{2}}\begin{bmatrix} S_{HH} + S_{VV} \\ S_{HH} - S_{VV} \\ 2S_{HV} \end{bmatrix}$$

The coherency matrix is computed as:

$$T_3 = \langle k_p k_p^{*T} \rangle$$

Where k_p denotes the Pauli target vector and k_p^{*T} represent the complex conjugate transpose. The coherency matrix representation enables extraction of physically meaningful scattering information from fully polarimetric SAR data

Image quality is further enhanced by applying a Lee Sigma speckle filter with a 7 × 7 window, effectively reducing speckle noise. Subsequently, seven component scattering power decomposition technique [7SD] is applied to extract physical scattering information, thereby yielding insights into the diverse land cover types present within the region. The extracted features are then used in the subsequent classification stage to distinguish between various land cover types.

2.3. Training Sample Selection

Five primary land cover categories were considered in this study: water, wetlands, forests, mangroves, and settlements. Representative training samples for each category were manually selected from the Mumbai dataset through visual interpretation of Pauli RGB composite and corresponding Google Earth reference imagery, as shown In Fig. 2.

The selected training regions were chosen to capture representative scattering behavior associated with each land cover category. Urban settlement samples were selected from dense built-up regions exhibiting strong double-bounce scattering characteristics, whereas forest and mangroves were identified based on dominant volume scattering response. Water bodies were selected from homogenous low-backscatter regions, while wetlands regions were identified using the transitional scattering patterns observed in coastal areas.

2.4. Classification

The classification process involves five primary land cover classes: water, wetlands, forest, mangroves, and settlements. Representative training samples are manually selected from the Mumbai dataset using visual interpretation of Pauli RGB composites and reference data from Google Earth imagery. Fig. 2a shows the Pauli RGB representation of ALOS2-PALSAR L-band data, while Fig. 2b presents the corresponding Google Earth image overlaid with ground truth samples for different land cover types. A Random Forest classifier, with user selected number of trees, is then trained using these samples obtained from Mumbai dataset.

The transfer learning concept in this study is achieved by applying the trained Mumbai-based classifier to geographically distinct datasets acquired from New Delhi, Ahmedabad, San Francisco, and California without retraining. Through this approach, the scattering properties and the classification properties learned through the data collected in Mumbai are applied in other geographic areas to test the ability of the classifier to perform well across different geographical regions.

The classified outputs generated from the model were further evaluated using confusion matrix-based analysis and subsequently utilized for land cover area estimation based on the spatial resolution of the ALOS2-PALSAR imagery.

2.5. Graphical User Interface

A MATLAB-based graphical user interface (GUI) has been constructed to enhance user-friendliness and facilitate the visualization of results (Fig. 3). This interface enables users to select a designated city and opt for one or several land cover categories from a checkbox-based list. Classes that are either inactive or non-existent are disabled, thereby ensuring an optimized user experience. The classified imagery is depicted utilizing a color-coded schema: blue representing water, cyan for wetlands, green indicating forests, red denoting settlements, and light green symbolizing mangroves. Classes that remain unselected are portrayed in black, thereby preserving visual clarity. Additionally, the GUI calculates and presents the distribution of land cover areas in square kilometers and incorporates functionality for the preservation of classified outputs.

3. RESULT

The classified image for the Mumbai dataset, which achieved an overall accuracy of 99.07% and a Kappa coefficient of 0.98, is shown in Fig. 4(b) alongside its corresponding Pauli RGB image in Fig. 4(a). The associated classification metrics are summarized in Table 1. To evaluate the generalizability of the trained

model, it was tested on datasets from San Francisco, California, Ahmedabad, and New Delhi. The classified outputs along with their respective Pauli RGB images are presented in Figs. 5 to 8. Additionally, a graphical user interface (GUI) was developed

to support user interaction and simplify the land cover classification workflow, as illustrated in Fig. 9. The GUI allows users to select one of five preconfigured urban areas—Mumbai, San Francisco, Ahmedabad, California, or Delhi—alongside one or more land cover classes: Water, Wetlands, Forest, Mangroves, or Settlements. The GUI also contains a text input field where users can specify the number of trees for the Random Forest classifier, thus offering user-adjustable model complexity. After selection, users can start the classification by clicking the "Execute" button. After

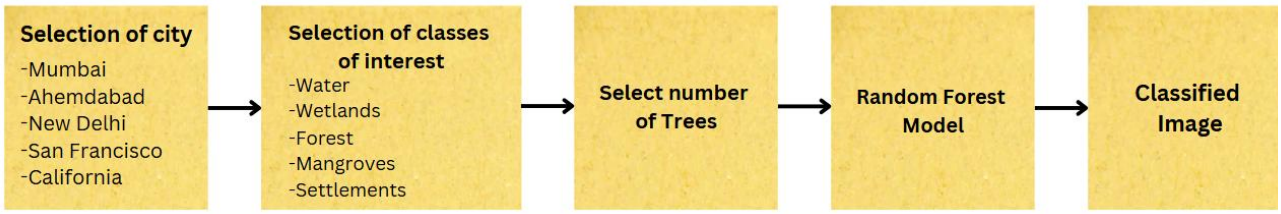

Fig. 3: Workflow of using Graphical User Interface

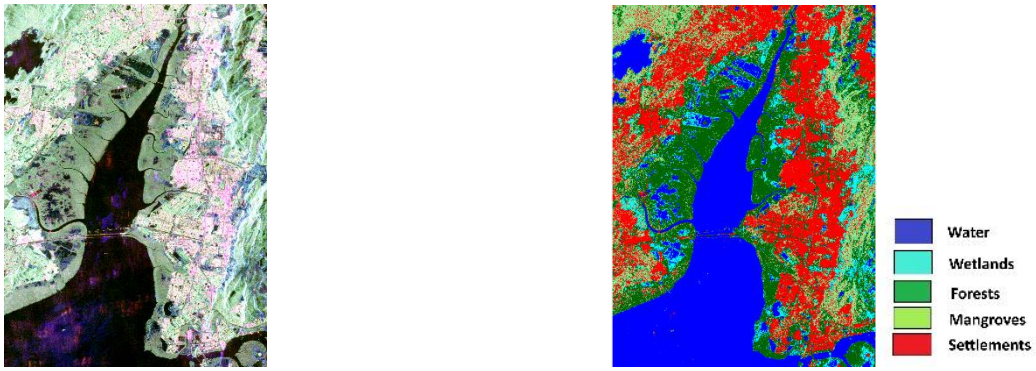

(a) (b)

Fig. 4: ALOS2-PALSAR L-Band Data for Mumbai: (a) Pauli RGB image, (b) Classified Image

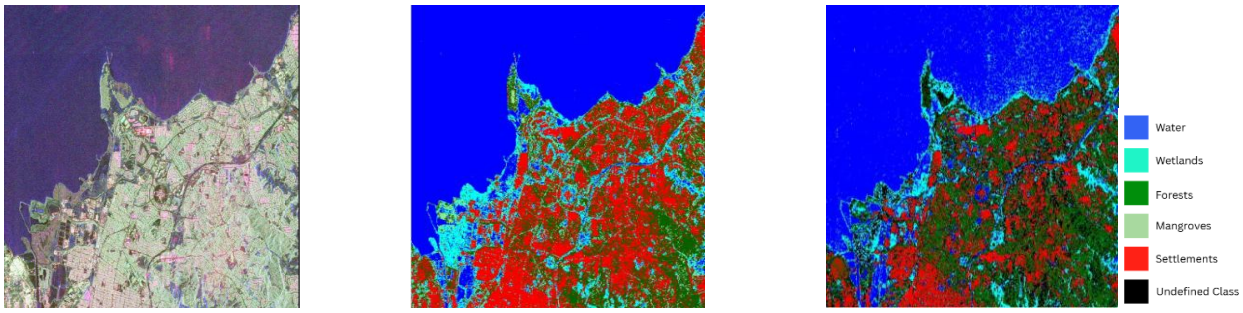

(a) Pauli RGB image

(b) Classified image after training on California Data (Accuracy – 99.78%)

(c) Classified image after training on Mumbai Data (Accuracy – 92.74 %)

Fig. 5. ALOS2-PALSAR L-Band California Data

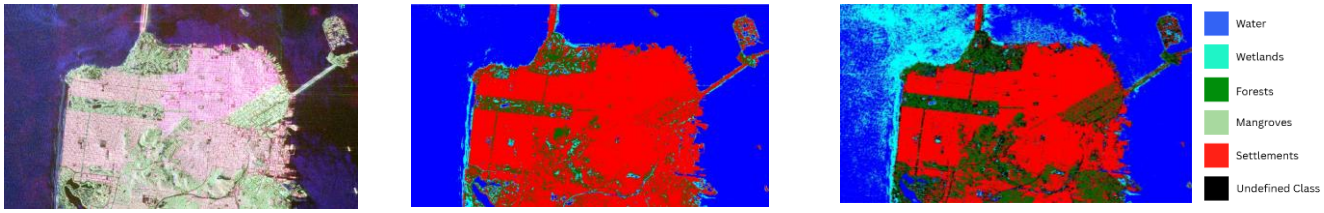

(a) Pauli RGB image

(b) Classified image after training on San-Francisco Data (Accuracy – 99.94%)

(c) Classified image after training on Mumbai Data (Accuracy – 90.31 %)

Fig. 6. ALOS2-PALSAR L-Band San Francisco Data

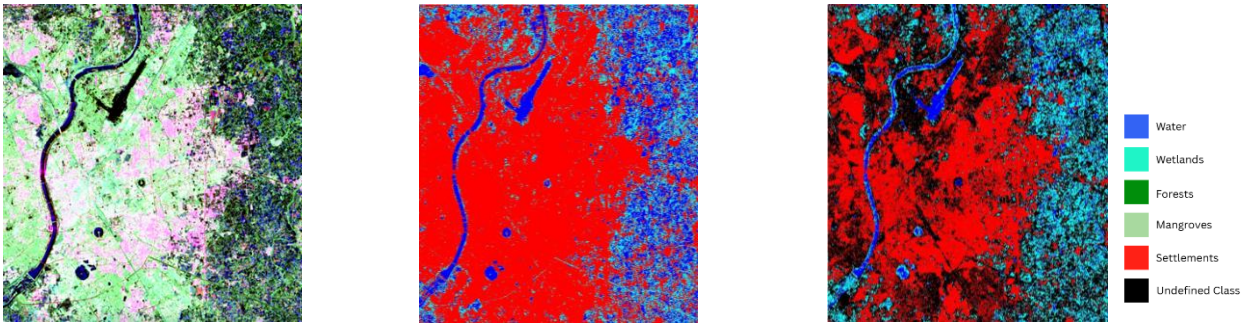

(a) Pauli RGB image (b) Classified image after training on Ahmedabad Data (Accuracy – 99.94%) (c) Classified image after training on Mumbai Data (Accuracy – 67.86 %)

Fig. 7. ALOS2-PALSAR L-Band Ahmedabad Data

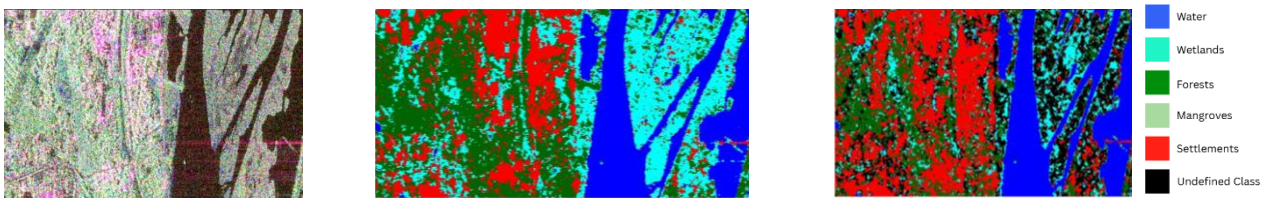

(a) Pauli RGB image (b) Classified image after training on New Delhi (Accuracy – 99.82%) (c) Classified image after training on Mumbai (Accuracy – 86.52%)

Fig. 8. ALOS2-PALSAR L-Band New Delhi Data

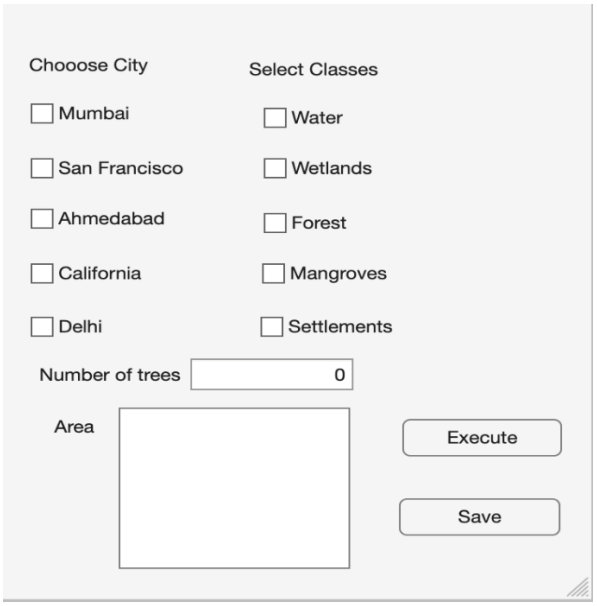

Fig. 9: Graphical User Interface

Table 1: Accuracy Metrics

Overall Accuracy	99.02%
Precision	0.98
Recall	0.98
F1 score	0.98
Kappa Coefficient	0.98

Table 2: Confusion Matrix (Training Accuracy – 99.0781%)

	Forest	Mangroves	Settlements	Water	Wetlands
Forest	95.9	1.6	2.2	0.1	0.2
Mangroves	0.1	99.4	0.1	0.1	0.2
Settlements	0.3	0.2	98.6	0.1	0.8

True Class

Water	0	0	0	99.9	0
Wetlands	0.5	1.2	1.3	0.1	96.9

Predicted Class

Table 3: Accuracy Comparison: Same-City Training vs. Mumbai-Based Training

Test City	Train = Same City	Train = Mumbai
Mumbai	99.23%	99.07%
San Francisco	99.94%	90.31%
California	99.78%	92.74%
Ahmedabad	99.74%	67.86%
New Delhi	99.82%	86.53%

the classification is complete, the "Area" panel displays the estimated land cover area (in square kilometers) for all selected categories. The "Save" button allows users to save the results for later documentation or analysis.

The confusion matrix (table 2) shows class-specific accuracies, precision, recall, and F1 scores of the classified Mumbai dataset. From table 3, when the model is trained and tested on the California dataset itself, it achieves accuracy of 99.78% while training and testing on the San Francisco dataset gives 99.94%. However, when the model trained on the Mumbai dataset is applied to these regions, accuracy drops to 92.74% and 90.31% respectively. This difference is expected because the model is optimized for the disoriented settlements and land cover characteristics of Mumbai. The differences in urban layout, vegetation types, and geographical features between cities contribute to this accuracy drop in cross-regional application. In the case of Ahmedabad and New Delhi, training and testing the model on their respective datasets results in high accuracies of 99.74% and 99.82%, respectively. However, when the Mumbai-trained model is applied, the accuracy declines to 67.86% for Ahmedabad and 86.53% for New Delhi. In both cases, a significant misclassification is observed, with agricultural fields frequently being incorrectly classified as forest, likely due to similarities in their backscatter characteristics. This misclassification can be attributed to the similarity in backscatter characteristics between certain types of dense vegetation in agricultural fields and forest areas. The L-band's ability to penetrate vegetation canopies may result in similar scattering mechanisms for both dense crops and forests. The model trained primarily on Mumbai's urban landscape with limited exposure to extensive agricultural areas, lacks the specific training data to accurately distinguish these agricultural fields from forest.

The usability of the tool was assessed through a user study comprising few participants. As illustrated in Fig. 10, a substantial majority (88.9%) possessed prior familiarity with remote sensing tools including PolSARPro, SNAP, QGIS, and ArcGIS, signifying a technically proficient user demographic. Concerning the classification workflow, Fig. 11 indicates that 91.7% of users appraised it as either clear (25%) or very clear (66.7%), thereby validating the logical progression and intelligibility of the procedure. In relation to the graphical user interface, Fig. 12 discloses that 66.7% of participants evaluated it as excellent, with an additional 27.8% categorizing it as good, thereby emphasizing the robust visual design and operational efficacy. As depicted in Fig. 13, 69.4% regarded the tool as highly user-friendly, while 25% deemed it user-friendly,

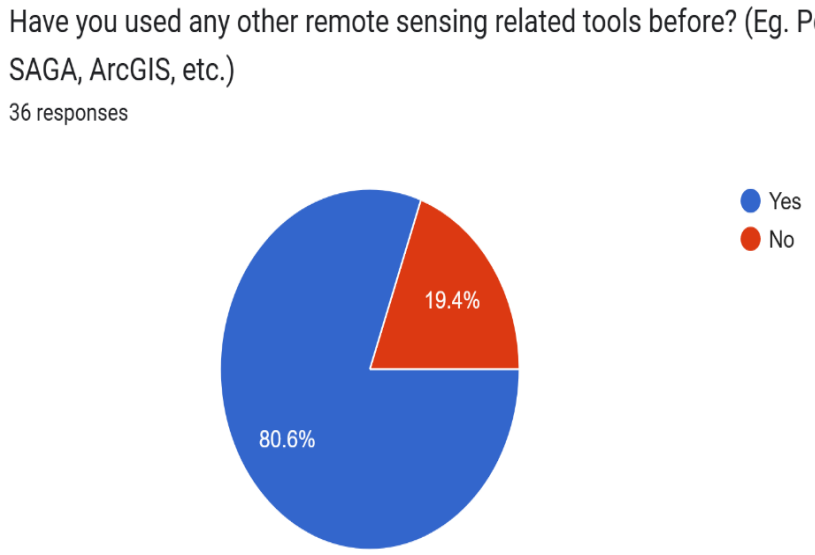

Fig. 10: Graph showing ease of use without prior remote sensing knowledge

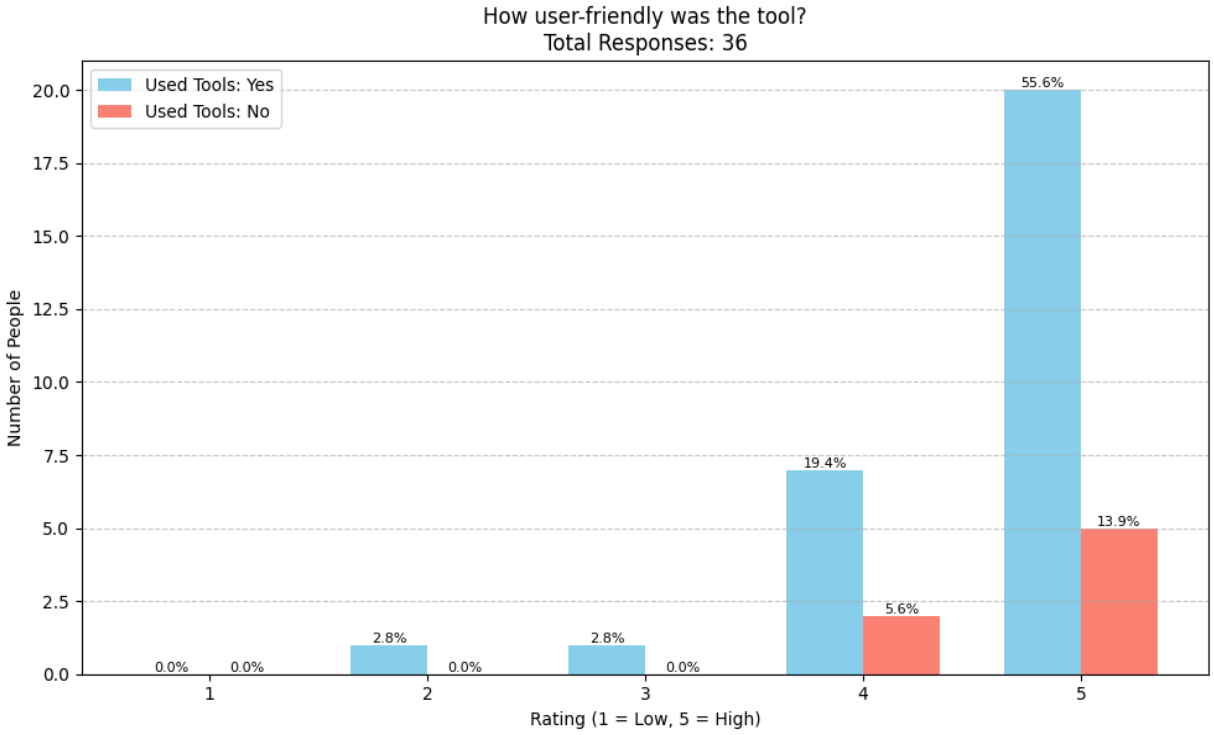

Fig. 11: Graph depicting user-friendliness ratings of the tool

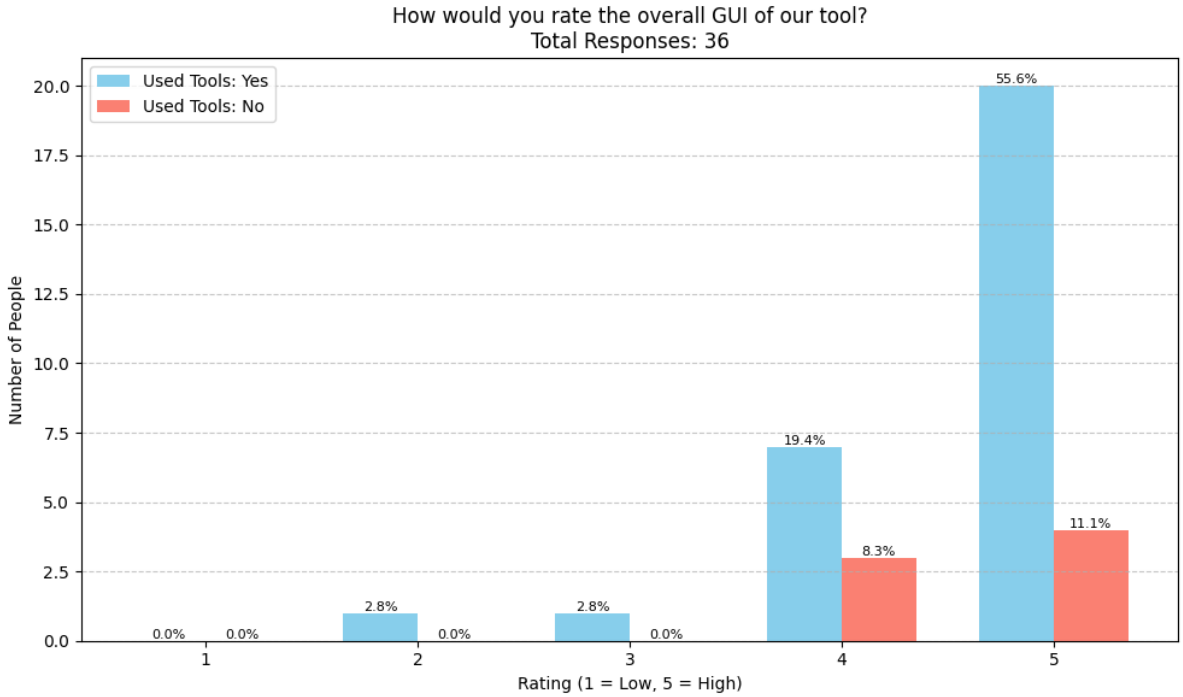

Fig. 12: Graph illustrating overall GUI ratings

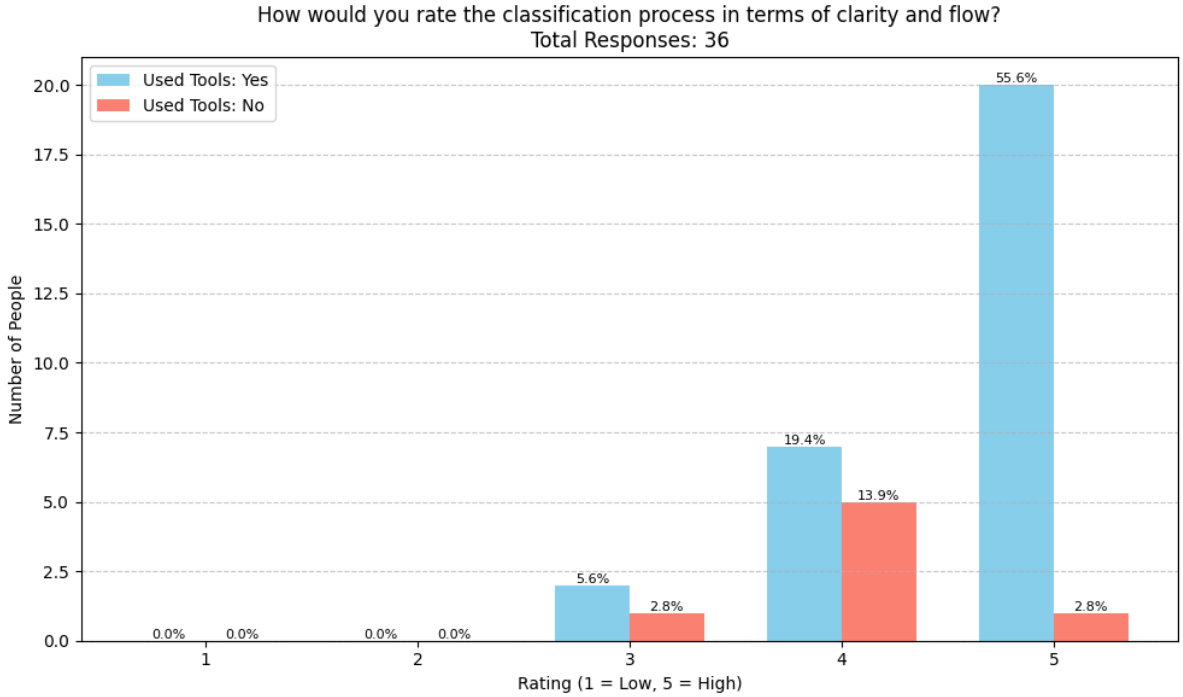

Fig. 13: Graph showing clarity and flow of the classification process

signifying that 94.4% of users experienced a favorable usability outcome. While region-specific training guarantees high accuracy, broader implementation may be gained from the inclusion of additional diverse training samples to address the complexities of varying land cover. In summary, the affirmative user feedback, intuitive design, and robust classification clarity substantiate the tool's promise for operational application in fields such as environmental monitoring and urban planning.

4. CONCLUSION

This research introduces a user-centric tool for land cover classification utilizing ALOS2-PALSAR L-band imagery, supported by a graphical user interface (GUI) to improve both accessibility and usability. The Random Forest classifier, which was initially trained using the Mumbai dataset, exhibited exceptional accuracy upon evaluation in the same geographic area (99.07%) and demonstrated relatively robust performance when applied to additional urban landscapes such as San

Francisco (90.31%) and California (92.74%). Nevertheless, a significant reduction in accuracy was recorded for Ahmedabad (67.86%) and New Delhi (86.53%), largely due to the misclassification of agricultural fields as forests. This misclassification can be attributed to the similarity in backscatter characteristics between certain types of dense vegetation in agricultural fields and forest areas, especially during growth stages or for certain crop types. The L-band's ability to penetrate vegetation canopies may result in similar scattering mechanisms for both dense crops and forests.

User evaluations derived from a usability study revealed that the tool is remarkably intuitive, with 91.7% of participants assessing the workflow as coherent and 94.5% finding it user-friendly irrespective of their prior experience. These outcomes substantiate the tool's relevance for a diverse array of users, encompassing urban planners, and academic researchers. Future research will aim to rectify existing limitations by integrating texture metrics such as Gray-Level Co-occurrence Matrix features, expanding the training repository with additional samples tailored to specific regions, and transitioning the platform to a cloud-based environment to facilitate large-scale, collaborative analyses. Through these advancements, the proposed system has the capacity to develop into a precise, scalable, and widely accessible solution for the monitoring of land covers utilizing PolSAR data.

5. ACKNOWLEDGMENTS

The authors would like to express their sincere gratitude to Dr. Gulab Singh for providing the dataset and for developing the decomposition technique employed in this study, which significantly contributed to the analysis. The authors also acknowledge the Japan Aerospace Exploration Agency (JAXA) for supplying the ALOS/PALSAR-2 L-band data for the New Delhi, Ahmedabad, California, and San Francisco test sites under RA Project No. RA6-3017, as well as the data for Mumbai under RA Project No. RA-305.

6. REFERENCES

[1] H. Parikh, S. Patel, and V. Patel, "Classification of SAR and PALSAR images using deep learning: a review," Int. J. Image Data Fusion, vol. 11, no. 1, pp. 1–32, 2019, doi: 10.1080/19479832.2019.1655489.

[2] E. Hossain, "App Designer and Graphical User Interface in MATLAB," in MATLAB and Simulink Crash Course for Engineers, Springer, Cham, 2022, doi: 10.1007/978-3-030-89762-8_11.

[3] B. Waske, S. van der Linden, C. Oldenburg, B. Jakimow, A. Rabe, and P. Hostert, "imageRF – A user-oriented implementation for remote sensing image analysis with Random Forests," Environ. Model. Softw., vol. 35, pp. 192–193, 2012, doi: 10.1016/j.envsoft.2012.01.014.

[4] M. Pal, "Random Forest classifier for remote sensing classification," Int. J. Remote Sens., vol. 26, no. 1, pp. 217–222, 2005, doi: 10.1080/01431160412331269698.

[5] S. S. Shinde and S. S. Patil, "Automatic land cover classification with SAR imagery and Machine learning using Google Earth Engine," International Journal of Electrical and Computer Engineering Systems, vol. 13, no. 10, pp. 909–916, Dec. 2022. doi: 10.32985/ijeces.13.10.6.

[6] R. Garg, A. Kumar, M. Prateek, K. Pandey, and S. Kumar, "Land cover classification of spaceborne multifrequency SAR and optical multispectral data using machine learning," Advances in Space Research, vol. 69, no. 5, pp. 1984–1997, Feb. 2022.

[7] J. Zhang, Y. Liu, Z. Wang, and Y. Li, "Land cover classification of SAR images based on ascending and descending orbit feature optimization and data fusion," 2025.

[8] L. Wang et al., "Research on land cover classification of multi-source remote sensing data based on improved U-net network," Scientific Reports, vol. 13, no. 1, Sep. 2023.

[9] S. Shetty et al., "MATSAR: A COMPREHENSIVE MACHINE LEARNING APPROACH FOR POLSAR DATA PROCESSING", International Journal of Computer Applications. 187. 23-29. 10.5120/ijca2025924824.

[10] P. O. Gislason, J. A. Benediktsson, and J. R. Sveinsson, "Random Forests for land cover classification," Pattern Recognition Letters, vol. 27, no. 4, pp. 294 300, Mar. 2006, doi: 10.1016/j.patrec.2005.08.011.

[11] A. Lapini, S. Pettinato, E. Santi, S. Paloscia, G. Fontanelli, and A. Garzelli, "Comparison of machine learning methods applied to SAR images for forest classification in Mediterranean areas," Remote Sensing, vol. 12, no. 3, p. 369, 2020. DOI: 10.3390/rs12030369.

[12] F. Zhang and X. Yang, "Improving land cover classification in an urbanized coastal area by random forests: The role of variable selection," Remote Sensing of Environment, vol. 251, p. 112105, 2020. DOI: 10.1016/j.rse.2020.112105.

[13] D. Ming, T. Zhou, M. Wang, and T. Tan, "Land cover classification using random forest with genetic algorithm-based parameter optimization," Journal of Applied Remote Sensing, vol. 10, no. 3, p. 035021, 2016. DOI: 10.1117/1.jrs.10.035021.

[14] M. Belgiu and L. Drăguţ, "Random forest in remote sensing: A review of applications and future directions," ISPRS Journal of Photogrammetry and Remote Sensing, vol. 114, pp. 24–31, Apr. 2016. doi : 10.1016/j.isprsjprs.2016.01.011

[15] F. F. Camargo, E. E. Sano, C. M. Almeida, J. C. Mura, and T. Almeida, "A comparative assessment of machine-learning techniques for land use and land cover classification of the Brazilian tropical savanna using ALOS 2/PALSAR-2 polarimetric images," Remote Sensing, vol. 11, no. 13, p. 1600, 2019. DOI: 10.3390/rs11131600.

[16] V. Turkar, Juhi Checker, Shaunak De, and Gulab Singh, "Impact of G4U and 7-component target decomposition on PALSAR image semantic segmentation," Advances in Space Research, vol. 70, no. 12, pp. 3798-3810, 2022, doi: 10.1016/j.asr.2022.08.004.

[17] G. Singh, R. Malik, S. Mohanty, V. S. Rathore, K. Yamada, M. Umemura, and Y. Yamaguchi, "Seven-Component Scattering Power Decomposition of POLSAR Coherency Matrix," IEEE Transactions on Geoscience and Remote Sensing, vol. 57, no. 11, pp. 8371–8382, Nov. 2019, doi: 10.1109/TGRS.2019.2920762.

[18] H. Fan, S. Quan, D. Dai, X. Wang, and S. Xiao, "Seven-component model-based decomposition for PolSAR data with sophisticated scattering models," Remote Sens., vol. 11, p. 2802, Nov. 2019

[19] W. Wang, X. Yang, G. Liu, H. Zhou, W. Ma, Y. Yu, and Z. Li, "Random forest classification of sediments on

exposed intertidal flats using ALOS-2 quad-polarimetric SAR data," Int. Arch. Photogramm. Remote Sens. Spatial Inf. Sci., vol. XLI-B8, pp. 1191–1194, 2016, doi: 10.5194/isprs-archives-XLI-B8-1191-2016.

[20] R. Kotru, V. Turkar, S. Simu, S. De, M. Shaikh, S. Banerjee, G. Singh, and A. Das, "Development of a generalized model to classify various land covers for ALOS-2 L-Band images using semantic segmentation," Advances in Space Research, vol. 70, no. 12, pp. 3811–3821, 2022, doi: 10.1016/j.asr.2022.07.078.

[21] V. Turkar, A. Masurkar, A. Das, and R. Daruwala, "Development of Generalized Machine Learning Model to Classify PALSAR Data," in IGARSS 2023 - 2023 IEEE International Geoscience and Remote Sensing Symposium, Pasadena, CA, USA, 2023, pp. 7475-7478, doi: 10.1109/IGARSS52108.2023.10281706.

[22] F. F. Camargo, E. E. Sano, C. M. Almeida, J. C. Mura, and T. Almeida, "A Comparative Assessment of Machine-Learning Techniques for Land Use and Land Cover Classification of the Brazilian Tropical Savanna Using ALOS-2/PALSAR-2 Polarimetric Images," Remote Sensing, vol. 11, no. 13, Art. no. 1600, 2019, doi: 10.3390/rs11131600.